January 2015

Warm Microhabitats Drive Both Increased Respiration and Growth Rates of Intertidal Consumers

Luke P. Miller
Stanford University, luke.miller@sjsu.edu

Bengt J. Allen
California State University - Long Beach

Felicia A. King
Stanford University

Daisy R. Chilin
California State University - Long Beach

Vanessa M. Reynoso
California State University - Long Beach

See next page for additional authors

Recommended Citation

Luke P. Miller, Bengt J. Allen, Felicia A. King, Daisy R. Chilin, Vanessa M. Reynoso, and Mark W. Denny. "Warm Microhabitats Drive Both Increased Respiration and Growth Rates of Intertidal Consumers" *Marine Ecology Progress Series* (2015): 127-143.

Warm microhabitats drive both increased respiration and growth rates of intertidal consumers

Luke P. Miller[1,*], Bengt J. Allen[2], Felicia A. King[1], Daisy R. Chilin[2], Vanessa M. Reynoso[2], Mark W. Denny[1]

[1] Hopkins Marine Station, Stanford University, Pacific Grove, CA, USA 93950

[2] Department of Biological Sciences, California State University Long Beach, Long Beach, CA, USA 90840

[*] corresponding author: contact@lukemiller.org

Running headline: Intertidal limpet respiration and growth

Abstract

Rocky intertidal organisms are often exposed to broadly fluctuating temperatures as the tides rise and fall. Many mobile consumers living on the shore are immobile during low tide, and can be exposed to high temperatures on calm, warm days. Rising body temperatures can raise metabolic rates, induce stress responses, and potentially affect growth and survival, but the effects may differ among species with different microhabitat preferences. We measured aerial and aquatic respiration rates of four species of *Lottia* limpets from central California, and estimated critical thermal maxima. In a variety of microhabitats in the field we tracked body temperatures and measured limpet growth rates on experimental plates colonized with natural microalgae. Limpet

species found higher on the shore had lower peak respiration rates during high temperature aerial exposure, and had higher critical thermal maxima. Using our long-term records of field body temperatures, we estimated cumulative respiration to be 5 to 14% higher in warm microhabitats. Growth rates in the field were driven by an interaction between available microalgal food resources, low tide temperature, and limpet species identity, with limpets from warmer microhabitats responding positively to higher food availability and higher low tide temperatures. Stressful conditions in warm microhabitats make up a small portion of the total lifetime of these limpets, but the greater proportion of time spent at non-stressful, but warm, body temperatures may enhance growth compared to limpets living in cooler microhabitats.

Keywords: intertidal zone, limpet, microalgae, shore height, temperature stress, thermotolerance

Introduction

Climate change research in a variety of aquatic systems has pointed to the potential for mildly increasing water temperatures to increase ectotherms' metabolic and foraging rates, and to increase the impacts of top-down control by consumers on resources (O'Connor 2009, O'Connor et al. 2009, Hoekman 2010, Kratina et al. 2012, O'Regan et al. 2014). As waters warm, the increasing speed of fundamental chemical reactions at the cellular level leads to increasing energy usage for maintenance metabolism and growth (Hochachka & Somero 2002) that must typically be balanced by increasing the rate of consumption, which in some cases can strengthen trophic cascades (Kratina et al. 2012). Provided there is room for acclimatization to a warmer temperature regime (Stillman 2003, Deutsch et al. 2008, Tewksbury et al. 2008), the rate of energy flow up through the trophic levels of the system could increase as species living below their optimum performance temperature move up the rising slope of their respective temperature

42 performance curves (Fig. 1A; Huey & Stevenson 1979), potentially driving greater productivity
43 (Angilletta et al. 2010).

44 In the rocky intertidal zone, the effects of benign water temperature fluctuations as
45 seawater warms and cools during high tide have been pointed to as potential benefits for some
46 intertidal consumers. Sanford and collaborators have shown that foraging rate increases within a
47 limited range of increasing water temperature for key intertidal species, including the keystone
48 predator *Pisaster ochraceus*, which increases its per capita predation on intertidal mussels that
49 are often the dominant competitors for space in the mid intertidal zone (Sanford 1999, Sanford &
50 Menge 2001, Sanford 2002, Pincebourde et al. 2008). Warmer waters can also increase intertidal
51 mussel growth (Phillips 2005, Kroeker et al. 2014) and speed up feeding rates in predatory snails
52 (Largen 1967, Bayne & Scullard 1978, Yamane & Gilman 2009, Miller 2013). However, those
53 are the rare cases for which we know where on the thermal performance curve an intertidal
54 organism sits relative to the range of varying temperatures experienced in its habitat. For other
55 organisms it is difficult to predict when or how often rising body temperatures could move the
56 organism from the ascending slope of the curve, past its optimum temperature, and onto the
57 descending slope. The distribution of temperatures experienced by intertidal organisms is
58 dominated by the influence of water temperature at high tide, while aerial exposure during low
59 tide can bring swings to either colder or warmer temperatures, as shown for high-intertidal-zone
60 limpets from Monterey Bay, California (Figure 1B). Most of these temperature fluctuations are
61 mild enough to avoid temperature stress (hatched region, Figure 1B, with the 28 °C upper limit
62 based on heat shock protein expression data from Dong et al. 2008), but occasional hot weather
63 conditions can drive body temperatures to extremes (gray region, Figure 1B), when low tides
64 leave marine organisms high and dry for hours at a time (Helmuth 1999, Denny & Harley 2006,

65 Denny et al. 2009). The temporal coincidence of warm water and air temperatures may also have
66 complicated interacting effects. Periods of cooler water temperatures at high tide have the
67 potential to offset negative effects of warm low tide conditions by providing time to recover
68 from stress, but periods with warm low tides and warm high tides occurring out of phase by
69 several days could have strong negative effects by leaving little time to recover (Pincebourde et
70 al. 2012).

71 Much of the climate-change related research in intertidal systems has focused on the
72 negative effects of increasing temperature, particularly on extreme aerial temperatures that
73 induce heat stress and occasionally cause mortality events during low tide (Tomanek & Somero
74 1999, Stillman 2002, Tomanek 2002, Muñoz et al. 2005, Jones et al. 2009, Miller et al. 2009,
75 Tomanek & Zuzow 2010, Miller et al. 2014). The assumption is often that low tide conditions,
76 when animals and algae are exposed to air, can drive species past their optimal temperature range
77 and down the descending slope of the temperature performance curve, with negative energetic
78 consequences derived from limited oxygen delivery or organ failure (Pörtner 2012) and the need
79 to shunt energy into heat shock responses to recover from high temperature insults (Feder &
80 Hofmann 1999). In addition, due to the physiological need for available water, most algal
81 photosynthesis and animal feeding occurs at high tide when body temperatures are at equilibrium
82 with the cool ocean. As the tide drops and the rocks dry, photosynthesis slows (Hunt & Denny
83 2008) and nearly all feeding activity comes to a stop (Craig 1968, Eaton 1968, Miller 1968). As a
84 result, the potential benefits of a warming body and faster metabolism that can occur in fully
85 aquatic systems are decoupled from the opportunity to feed or photosynthesize for the many
86 sessile, or functionally-sessile, organisms in the intertidal zone during low tide.

87 The cessation of feeding does not necessarily mark the end of energy acquisition, since
88 digestion of a meal may take hours, and those hours may include warm daytime low tide
89 conditions. In aquatic habitats, when food is abundant, the temperature for optimal growth in
90 ectotherms can increase (Elliott 1976, Elliott 1982, Stich & Lampert 1984, Pangle & Peacor
91 2010), and warmer temperatures can increase the rate of digestion (Brett & Higgs 1970,
92 Diefenbach 1975, Bayne & Scullard 1978). However, in the intertidal zone where food
93 availability or foraging time may be restricted, the scope for growth will be lower and there can
94 be an expanded range of high temperatures where metabolic maintenance costs outstrip energy
95 intake (Woodin et al. 2013, Iles 2014). Therefore, along the seashore, it remains an open
96 question as to whether warm, dry conditions during daytime low tides are a potential benefit or
97 simply a cost for consumers and their algal resources, though some studies show that the effects
98 of warm temperatures at low tide need not be solely negative (Gilman 2006, Blanchette et al.
99 2007).

100 We address this question using limpets in the genus *Lottia* found on the central coast of
101 California. In rocky intertidal zones around the world, limpets represent an important class of
102 herbivorous grazers that can structure the intertidal community by selectively removing algae
103 and settling invertebrates (Jones 1948, Branch 1981, Hawkins & Hartnoll 1983). Limpets forage
104 while the rocks are awash during rising and falling high tides, and typically remain fixed in place
105 on the rock during low tide when the sea recedes (though some tropical species move with the
106 tides, Williams & Morritt 1995). This foraging pattern often precludes any sort of shelter-seeking
107 behavior when low tide environmental conditions might generate temperature and desiccation
108 stress. Unlike more mobile species that could shuttle between different thermal microhabitats to
109 control body temperature near some optimum performance peak (Huey 1991, Hertz et al. 1993,

110 Allen & Levinton 2014), limpets are functionally sessile at low tide and their body temperatures
111 can exceed the optimum temperature range, in some cases inducing sublethal or lethal stress
112 (Dong et al. 2008). While the rock is dry there is no opportunity to graze microalgae, but there is
113 some indication that digestion may continue during low tide periods (Walker 1968; L. Miller
114 personal observation). Limpets are ideal for studies of temperature effects, as their large foot
115 keeps them tightly thermally coupled to the underlying substratum, so that temperature
116 measurements of the substratum can act as accurate proxies for limpet body temperature without
117 disturbing the organism (Wolcott 1973, Denny & Harley 2006).

118 The four *Lottia* species utilized in this study differ in their preferred shore height and
119 microhabitat (Figure 2). The vertical distributions of the four species overlap to some extent, but
120 they are often found in distinct microhabitats. *L. pelta* Rathke and *L. limatula* Carpenter are
121 found in the low and mid intertidal zone, with *L. pelta* favoring wave-exposed walls or mussel
122 beds where it consumes both microalgae and macroalgae, while *L. limatula* is often found on
123 more sun-exposed horizontal surfaces and feeds primarily on microalgae (Craig 1968, Eaton
124 1968, Wolcott 1973). *L. scabra* Gould and *L. austrodigitalis* Murphy are found higher on the
125 shore, above the *Mytilus californianus* mussel zone and often above the limits of the *Endocladia*
126 *muricata* macroalgal zone (Wolcott 1973). Both high-zone species are found on vertical walls,
127 but *L. scabra* is also found on horizontal, sun-exposed rocks where *L. austrodigitalis* is often
128 absent (Collins 1976, Hahn & Denny 1989). *L. austrodigitalis* is the highest ranging limpet on
129 the central California coast, often found more than five meters above Mean Lower Low Water
130 (MLLW) on wave-exposed rock walls (Miller 1968) in a region where the maximal still-water
131 tidal range is approximately 2.5 m.

In Monterey Bay, *L. austrodigitalis* overlaps with a cryptic congener, *L. digitalis* Rathke, which can only reliably be distinguished via genetic methods, but the two species share similar behaviors and occupy the same microhabitats (Murphy 1978, Crummett & Eernisse 2007). Recent work at our field site at Hopkins Marine Station (HMS hereafter, Pacific Grove, CA, 36.6217N 121.9043W) has shown that *L. austrodigitalis* makes up the majority (88-89%) of the population of the cryptic species pair living on high shore rock habitats where we sampled (Dong et al. 2008, Dong & Somero 2009). This work also indicates that the two species overlap in their median upper thermal tolerance limits, with *L. austrodigitalis* being marginally more tolerant and producing more thermally stable cytosolic malate dehydrogenase (Dong & Somero 2009). We refer to *L. austrodigitalis* hereafter in this study while acknowledging that a small fraction of our samples may include *L. digitalis*.

To explore the potential effects of sub-lethal temperature variation on intertidal limpets, we measured respiration rate across a range of temperatures under aquatic and aerial conditions in the laboratory and tracked growth in the field while measuring microhabitat temperature and microalgal food supply. We looked for evidence of physiological compensation for increasing temperatures via reductions in the Q_{10} response of respiration (Q_{10} is defined as the ratio of the rates of a physiological or biochemical process over a 10 °C rise in temperature, where the common expectation is for a doubling of the rate, $Q_{10} = 2$, Hochachka & Somero 2002), and measured upper critical thermal maxima during aerial exposure. We expected to find increasing respiration rates with increasing body temperatures, such that field microhabitats with warmer low tide temperatures could either yield reduced limpet growth due to greater energetic demands, or increased growth if sufficient food was available to support higher metabolic rates. We

hypothesized that high shore and low shore limpets would differ in their response to warmer low tide temperatures, with high shore species being better adapted to cope with higher temperatures.

Methods

Collections

We collected the four species of limpets: *L. scabra, L. austrodigitalis, L. limatula*, and *L. pelta*, from south- and east-facing rocks at HMS during September and October 2013. The individuals collected for the trials were representative of the range of sizes of sub-adult and small adult limpets found at HMS for each of the four species (Table S1). Batches of limpets were collected and held in a shaded seawater table for 2 to 7 days prior to use in the respiration trials. Temperature in the seawater table was monitored with an iButton temperature logger (DS1921G, Maxim Integrated, San Jose, CA, USA) and remained at 15 °C during the experimental period.

Respiration trials

The respiration chamber consisted of a custom-machined aluminum block with 15 wells of 15 ml volume each, and a bolt-on top plate that contained ports for purging the chambers and making oxygen measurements. The block was submerged in a digitally-controlled water bath to maintain temperatures during trials. Oxygen measurements were taken using ruthenium sensor dots adhered to a glass port in the top plate for each well (aerial trials: RedEye patch, Ocean Optics, Dunedin, FL, USA; aquatic trials: SP-PSt3-NAU-D5-YOP, PreSens Precision Sensing GmbH, Regensburg, Germany) and read with a fiber-optic fluorescence-based optode system (NeoFox, Ocean Optics). The chamber top plate contained machined recesses and an indexing pin to ensure that the optode was placed at the same height and incident angle relative to the sensor patch for every reading, since deviations in positioning will substantially alter the signal

produced by the optode measuring system. Each oxygen sensor dot was recalibrated following each replicate trial using water-saturated normoxic air and pure CO_2 at the corresponding experimental temperature to make a two point calibration.

Aerial respiration

For aerial respiration trials, we reduced the volume of each chamber to 5 ml by inserting a 10 ml aluminum plug in the bottom of each well. 12 limpets, three per species, were run in individual wells along with three empty (blank) wells for each replicate trial. Each well also contained a 5 mm diameter piece of paper towel wetted with seawater to maintain 100% relative humidity during the trial. The aluminum block was initially held at 15 °C for 20 min, and the temperature of the water bath and block was then raised or lowered at a rate of 10 °C h^{-1} to the target experimental temperature for each trial. A total of 9 experimental temperatures were used in the aerial trials: 10, 15, 20, 25, 30, 32.5, 35, 37.5, and 40 °C. The time during the ramp to lower and higher temperatures allowed limpets to acclimate to the chamber, while for trial temperatures of 15 °C we waited 30 min before beginning the measurement process (equivalent to the minimum acclimation period for the 10 and 20 °C trials). The top plate of the chambers was bolted on and ports sealed to begin a 2 h measurement period. During the sampling period, the fiber optic sensor for the optode system was moved to each chamber well in succession for a 15 s reading, and each well was sampled every 8 min. The 2 h exposure allowed sufficient time for limpets to deplete a measurable amount of oxygen even at the lowest temperatures.

Aquatic respiration

The full 15 ml volume of the respiration chamber wells was used for the aquatic trials. We used artificial seawater (Instant Ocean, Blacksburg, VA, USA) mixed to a practical salinity of 33 to fill each chamber. Seawater was equilibrated to 15 °C and aerated before filling the

chambers. As in the aerial respiration trials, a single limpet was placed in each well, with three representatives of each of the four species filling 12 of the chamber wells, along with three empty (blank) wells. Aquatic temperature trials took place at 10, 12.5, 15, and 17.5 °C, to cover the range of typical seawater temperatures found through the year at HMS. The temperature of the chambers was changed at 10 °C h^{-1}, and a minimum acclimation period of 30 min was given for trials that took less than 30 min to reach the experimental target temperature (12.5, 15, and 17.5 °C trials). We used the 10 °C h^{-1} rate of water temperature change to harmonize our trial run times with those of the aerial respiration trials, and although our largest shift in water temperature did not exceed 5 °C, it should be noted that this rate of water temperature change is faster than the rate of natural water temperature shifts at this field site. Immediately prior to closing the chambers, we flushed each chamber with aerated seawater, pre-equilibrated to the experimental temperature. Prior to taking a reading in each chamber, the water was stirred manually for 20 s with a stir rod mounted in one of the top ports. Readings were taken for 15 s, and each chamber was sampled every 8 min for 1 h. We chose this shorter trial time to avoid limpets depleting oxygen in the water.

Processing respiration data

Immediately following a respiration trial, we weighed each limpet to the nearest 0.1 mg, in air and submerged in seawater. The displaced mass of the live limpet in seawater was used to calculate the volume that the limpet occupied in a chamber well. The volume of air or seawater in the chamber (minus the volume of the limpet) was used to calculate the volume of oxygen present at each time point. For aquatic trials, the concentration of O_2 in seawater (mg l^{-1}) was calculated using the temperature and salinity values for the trial with the relationship from Benson and Krause (1984), and converted to µmol of O_2 using the volume of seawater in the

chamber. We fit a linear regression to the µmol of O_2 through time to estimate the O_2 consumption rate. The values from the blank control chambers were averaged and used to correct for any drift that occurred during a trial. We dissected the tissue from the shell of each limpet and dried it in a drying oven at 60 °C for 48 h. The dry tissue mass was used to calculate the mass-specific oxygen consumption rate for each limpet. Each limpet was used in only a single temperature trial, and a total of 12 replicate limpets were used at each of the experimental temperatures for each species. We estimated Arrhenius break temperatures for log-transformed respiration rate with a piecewise regression using the R package *segmented* (Muggeo 2008).

We calculated Q_{10} values for aerial respiration rate across each successive pair of temperatures in the experiment using the equation

$$Q_{10} = \left(\frac{Rate_2}{Rate_1}\right)^{\frac{10}{Temp_2 - Temp_1}}.$$

To calculate 95% confidence intervals on this estimate, we used a bootstrap resampling procedure on each pair of 12 respiration values at two temperatures to produce a distribution of log-transformed Q_{10} estimates that better accounts for potential skew in the calculated values than a standard error estimate based on the assumption of normality (Davison & Hinkley 1997).

Heat coma temperatures in air

At the conclusion of each aerial respiration trial, we probed each limpet to determine if it was still adhered to the chamber wall. Any limpet that was poorly adhered and had also retracted the mantle tissue back from the edge of the shell was judged to be in heat coma. We fit a logit-link binomial generalized linear model to calculate the median heat coma temperature, termed the Critical Thermal Maximum, CT_{max}, for each species after 2 h at the experimental temperature.

244 *Field growth experiment*

245 In June 2013, we deployed a series of experimental plates in the rocky intertidal zone at
246 HMS to track limpet growth in various thermal microhabitats. Each plate was made of
247 aluminum, 10 cm diameter and 12 mm thick, topped with a layer of light gray rubber grip tape
248 (Safety Walk Tape, 3M, St. Paul, MN, USA). A 20 mm tall stainless steel mesh fence with 5.5
249 mm square openings was attached around the outer perimeter of the plate to dissuade limpets
250 from crawling off the plate. We machined a pocket into the underside of each aluminum plate to
251 hold an individually calibrated, wax-coated, iButton temperature datalogger with a resolution of
252 0.5 °C (DS1921G, Maxim Integrated, San Jose, CA, USA). The high thermal conductivity of
253 aluminum, the close proximity of the iButton to the upper surface of the plate, and the high
254 conductive heat exchange between the substratum and the large foot of a limpet allowed us to
255 use the iButton temperature as a direct proxy for the body temperature of the limpets attached to
256 the plate without disturbing the organisms (Wolcott 1973, Denny & Harley 2006). The iButtons
257 recorded temperatures in each plate every 12 minutes; we downloaded the data every two weeks.

258 We attached the experimental plates to the granite bedrock at HMS using a single bolt
259 through the center of the plate, and ensured good thermal contact with the underlying rock by
260 installing a thin layer of concrete between the plate and rock surface to fill surface irregularities.
261 Each plate held four individuals from one of the four species of *Lottia* described above, and we
262 deployed additional plates without limpets to serve as grazer exclusion controls. The resulting
263 density of 0.5 limpets cm^{-2} is similar to values measured for natural high shore *L. scabra*
264 populations and lower than densities of limpet populations lower on the shore (Sutherland 1970,
265 Morelissen & Harley 2007). A total of twelve plates per species (48 plates with limpets + 12
266 grazer exclusion plates) were placed on sloped or vertical surfaces at 1.4 or 1.7 m above Mean

Lower Low Water in horizontal transects at six sites. The sites included wave-exposed and wave-protected microhabitats that faced predominantly north, east, or west, encompassing much of the variety in microhabitats occupied by these species at HMS. The limpets were collected from surrounding rocks and individually tagged with numbered bee tags (The Bee Works, Orillia, ON, Canada) and cyanoacrylate glue. When limpets were lost from plates during the experiment, they were replaced to keep the total number of limpets on each plate at four. Missing limpets typically crawled over the fences and re-established on the surrounding rock face, and the different species showed difference propensities for escaping, with an average of 0.11 ± 0.15 (1 SD) *L. scabra*, 0.70 ± 0.42 *L. limatula*, 1.12 ± 0.85 *L. pelta*, and 1.31 ± 0.94 *L. austrodigitalis* limpets leaving per plate per census period. It should be noted that *L. scabra* typically establishes a home "scar" and grows the margin of the shell to fit the contours of the rock (Wolcott 1973). That tight fit was lost when we placed *L. scabra* on our plates, and it is possible that this may have affected desiccation rates and energy expenditures initially. We observed that *L. scabra* quickly established new home scars on the plates, and new shell growth matched the margins of the shell to the flatter surface of the experimental plate by the next census date.

Following the initial deployment on June 17, the limpets on each plate were censused on July 10, August 6, September 6, October 6, November 6, and December 1, 2013 as tide cycles and wave conditions allowed. We tracked limpet growth using digital photographs taken from overhead on each plate with a framer designed to keep a constant height and orientation to the plate, so that we could measure the projected area of each limpet shell to 0.1 mm^2 using ImageJ (Rasband).

We used a PAM fluorometer (Diving-PAM, Walz GmbH, Effeltrich, Germany) to track microalgal densities on the experimental plates. Microalgae were allowed to settle naturally from

290 the ocean for one month prior to the start of data collection. During night time low tides
291 associated with each limpet census, we took six haphazardly arrayed readings on each plate of
292 dark-adapted fluorescence (F_o), which serves as a non-destructive proxy for microalgal
293 chlorophyll *a* density (Barranguet & Kromkamp 2000, Honeywill et al. 2002, Serôdio et al.
294 2008). The tip of the fiber-optic measuring head of the fluorometer was fitted with a 10mm
295 spacer to maintain a fixed distance from the plate surface, and the opening covered an area of 53
296 mm^2. The tip was held in place at each measurement site until the F_o value stabilized (typically
297 3-5 seconds) before recording a value, as recommended by the manufacturer. As the amount of
298 surface moisture can affect F_o values (Maggi et al. 2013), we restricted sampling to periods when
299 the plates were moist, but not actively splashed or submerged by the tide.
300 We used a generalized least squares linear model from R package *nlme* (Pinheiro & Bates
301 2000) to assess the relationship between $\log_e$-transformed algal fluorescence (F_o) during each
302 census period and average daily maximum temperature, with limpet species (or grazer exclusion
303 plates) as a fixed factor. The temporal correlation of F_o values on individual plates across the
304 census periods was incorporated using a AR(1) autoregressive correlation structure (Pinheiro &
305 Bates 2000). A fixed effect of shore level (1.4m or 1.7m) was initially included in the model, but
306 was non-significant based on likelihood ratio tests, so it was removed from the final model, and
307 plates from both shore heights were pooled. For the model of limpet growth rate (shell + tissue
308 mass change relative to initial mass, mg day^{-1}) in each census period, we used a linear mixed
309 effects model to evaluate the interacting fixed effects of average daily maximum temperature
310 during a census period, our proxy for log-transformed algal density (F_o) at the start of each
311 census period, and limpet species identity (n = 1152 observations among 359 limpets across 6
312 census periods). The model included a random effect for plates and a random effect for

313 individual limpets nested within plates to account for nesting and for repeated measures of
314 individual limpets across census periods. Log-transformed F_o from the start of each census
315 period was also included as a random covariate to account for temporal autocorrelation, and the
316 model included an AR(1) correlation structure for the random factors. While there are numerous
317 ways to describe the temperature conditions in the field, we used the average daily maximum
318 temperature during a census period to summarize the differences between plates deployed in
319 different microhabitats. Model residuals were checked for normality and for evidence of
320 heterogeneity of variances. All analyses were carried out in R 3.1.1 (R Development Core Team
321 2014).
322
323 *Estimating cumulative respiration*
324 Using the temperature records from a subset of experimental plates and the data from our
325 respiration trials, we estimated the cumulative respired O_2 of an average sized limpet of each
326 species on the coolest and warmest plates (2 plates per species) on which that species was
327 present in the field experiment, for the entire period from June to December 2013. We chose to
328 use the single lowest variation and single highest variation plate for each species to encompass
329 the full range of temperature variation the limpets might have experienced in the field
330 experiment. Because the experimental plates were alternately submerged and emersed by the
331 tides, we used NOAA tide records for Monterey, CA to determine when plates were likely
332 submerged at high tide, and used respiration rates from the aquatic respiration trials for those
333 time periods. All other time periods used the aerial respiration data. The respiration rate at a
334 given temperature (μmol O_2 hr^{-1} g^{-1} dry tissue mass) was multiplied by the dry tissue mass of a
335 representative average sized limpet of each species and assumed constant for a 12 minute

interval to estimate the respired μmol of O_2 for each time step. When the temperature for a time point fell between two of the respiration trial temperatures, we used linear interpolation between the two closest trial temperatures to estimate respiration at the intermediate temperature. For any temperatures that fell below the limits of our respiration trial temperatures, we used the respiration rate value for the lowest trial temperature.

Results

Respiration

All four species of *Lottia* limpets showed an increase in aerial respiration rate as temperatures rose until reaching a peak temperature after which respiration dropped as limpets entered heat coma (Figure 3A, closed symbols). *L. scabra*, the high shore species often found in sun-exposed horizontal microhabitats, had the highest temperature of peak respiration at 37.5 °C. The high-shore, vertical-wall-favoring species *L. austrodigitalis* and the low-shore sun-exposed *L. limatula* both had a peak respiration rate near 35 °C. The low-shore species *L. pelta*, which favors cooler wave-exposed vertical walls, had the lowest peak respiration temperature at 32.5 °C. By 40 °C all of the species exhibited a decline in respiration rate, likely indicative of heart failure and heat coma (Bjelde & Todgham 2013). Our range of trial temperatures and the high peak temperature of respiration for *L. scabra* did not allow for a proper estimation of a break temperature for that species, but the break temperatures of the other species were lower than the likely break point for *L. scabra* near 37 °C (Table 1). All four species exhibited their highest Q_{10} values between 10 and 20 °C (4.3 for *L. scabra*, 2.3 for *L. austrodigitalis*, 2.9 for *L. limatula*, and 2.2 for *L. pelta*, Figure 3B). Each species showed a relaxation in Q_{10} to the 1.1 – 1.5 range between 20 °C and 30 °C, with a brief increase in Q_{10} prior to the peak respiration temperature.

For the narrower range of water temperatures used in the aquatic trials, changes in respiration rate were much smaller than the aerial trials (Figure 3A, open symbols) with overlapping 95% confidence intervals at all temperatures from 10 to 17.5 °C. Three of the species, *L. scabra*, *L. austrodigitalis*, and *L. limatula*, had aquatic respiration Q_{10} values between 2.0 and 2.2 over the 10 to 17.5 °C range, while *L. pelta* had a lower Q_{10} of 1.4.

Heat coma temperatures

Each of the four limpet species exhibited symptoms of heat coma at the highest aerial respiration trial temperatures (Table 1), and there were significant differences in median CT_{max} between species (Analysis of deviance for Temperature $\chi^2 = 218$, df = 1, $P < 0.001$; Species $\chi^2 = 43.9$, df = 3, $P < 0.001$). The two high shore species, *L. scabra* and *L. austrodigitalis* had significantly higher median CT_{max} values than the low shore species (*L. scabra* = *L. austrodigitalis* > *L. limatula* > *L. pelta*, Tukey post-hoc tests, $P < 0.05$). All *L. limatula* and *L. pelta* had entered heat coma at 40 °C, while some representatives of *L. scabra* and *L. austrodigitalis* remained adhered and responsive at the conclusion of the 2 h exposure even at the highest temperature in the experiment.

Field growth experiment

The ANCOVA analysis of log-transformed dark-adapted fluorescence F_o, our proxy for algal density, showed a non-significant interaction between average daily maximum temperature and limpet species identity ($F_{4, 350} = 1.89$, $P = 0.111$), but there was a significant main effect of limpet species identity ($F_{4, 350} = 80.8$, $P < 0.001$) and the average daily maximum temperature covariate ($F_{1, 350} = 104.3$, $P < 0.001$, Table S2). Coefficient estimates for the model are given in Table S3. Tukey post-hoc tests of the main effect of limpet species (including grazer exclusions) show that the intercepts for all four limpet species treatments were significantly lower than the

grazer exclusion plates, while *L. pelta* and *L. scabra* were not significantly different from each other, nor were *L. limatula* and *L. austrodigitalis*. Limpet grazing reduced the amount of algae on plates relative to grazer exclusions, but did not change the slope of the negative relationship between algal density and average daily temperature range found on all plates (Figure 4).

Using the regression values for limpet mass vs. projected area in the census photographs (Table S4), we were able to track limpet growth non-invasively on the experimental field plates through the experiment. There was a significant three-way interaction between average daily maximum temperature during a census period, log-transformed algal fluorescence at the start of each census period, and limpet species identity (Table 2, $F_{3, 671} = 8.12, P < 0.001$). Partial effects plots for the 3-way ANCOVA (Fox & Weisberg 2011) revealed that predicted limpet growth rate remained flat or increased with increasing average daily maximum temperature across a range of representative F_o values, but that the slope of the relationship differed among limpet species and F_o levels (Figure 5; coefficient estimates given in Table S5).

Estimated respiration in the field

The experimental plates deployed in the field at HMS showed a 3-fold variation in average daily temperature range from the coolest to warmest plate for each species, and a 9 to 13°C difference in maximum temperatures (Figure 6A, Table 3). Using the temperature data from the coolest and warmest plates for each species, we predicted a 5 to 14% increase in cumulative respired µmol O_2 for average sized limpets living on the warmest plates (Figure 6B and Figure 6C, Table 3) over the entire experimental period, relative to the coolest plate. None of the plates exceeded the estimated CT_{max} thresholds for any of the species during the 24 weeks of the experiment.

Discussion

All four species of *Lottia* limpets exhibit a large increase in respiration rate with increasing temperature while aerially emersed. In seawater temperatures within the normal yearly range for HMS (10 – 17.5 °C), respiration rates are typically in the range of 8 to 18 µmol O_2 h^{-1} g^{-1} (dry tissue mass), but when limpets are exposed to body temperatures in air within the range of extremes found at low tide, their peak respiration rates range from 30 to 60 µmol O_2 h^{-1} g^{-1}. At low temperatures there was substantial overlap in aerial and aquatic respiration rates, though the trend for increasing respiration rate in water appears lower than in air. A lower overall respiration rate in water at higher temperatures has been observed in *L. digitalis* (Bjelde & Todgham 2013), but other intertidal species such as *Pisaster* seastars show the opposite pattern, with higher aquatic respiration rates than aerial respiration rates at the same temperature (Fly et al. 2012).

We see some evidence for differential respiration responses and susceptibility to heat stress while emersed between the low shore species (*L. pelta* and *L. limatula*), and the high shore species (*L. austrodigitalis* and *L. scabra*). Both high shore species have higher median CT_{max} values and maintain slightly lower aerial respiration rates from 25 to 32.5 °C than the low shore species. *L. pelta*, the low shore species that is typically found on vertical faces, in wave-exposed microhabitats, or hiding under algal cover, is the least tolerant of prolonged aerial emersion at high temperatures and had the lowest CT_{max} and lowest temperature of peak respiration, though interestingly it also maintains a relatively high aerial respiration rate at temperatures common in those cool microhabitats. It may be the case that *L. pelta* is particularly adapted to maximizing metabolism and growth in cool microhabitats, at the cost of reduced tolerance to higher temperatures. The second low shore species, *L. limatula*, which inhabits similar microhabitats as

426 *L. pelta* but is also often found on horizontal, sun-exposed rocks in the low and mid-shore zone,
427 shows the most drastic increase in aerial respiration rate, increasing nearly 6-fold over the 10 to
428 35 °C range. Both low shore species had estimated respiration break points within one degree of
429 their median CT_{max} values, so that the range of temperatures where maximum respiration rate
430 occurred was followed closely by the onset of heat coma. In contrast, *L. austrodigitalis*, which is
431 the highest-living limpet species on the shore at HMS, limits its respiration rate increase to half
432 that of *L. limatula* across that same temperature range, perhaps reflecting a need to limit energy
433 expenditure during the frequent prolonged aerial emersion periods that come from living high on
434 the shore and the reduced availability of algal food resources to support a high metabolic rate.
435 The CT_{max} for *L. austrodigitalis* was 4 °C higher than the estimated respiration break point
436 temperature, indicating that this high shore species can maintain attachment to the rock and
437 avoid signs of heat coma longer after its respiration has begun to falter. The other high shore
438 species, *L. scabra*, is typically found in warmer microhabitats than *L. austrodigitalis*, living on
439 horizontal, sun-exposed rocks that occasionally reach the highest intertidal temperatures at HMS.
440 While *L. scabra* exhibits a slightly higher respiration rate than *L. austrodigitalis*, the peak rate
441 occurs at a slightly higher temperature, and is accompanied by a slightly higher CT_{max}, indicating
442 greater thermotolerance.

443 Each of the limpet species shows some evidence of metabolic rate control as they move
444 through the 20 to 30 °C temperature range, which is the most common range of warm, but not
445 extreme, daytime low tide rock temperatures at this site (Denny et al. 2006, Miller et al. 2009).
446 Q_{10} values for this temperature range typically remain below 1.5, lower than the expected value
447 of 2 to 3 for many temperature-dependent metabolic processes (Hochachka & Somero 2002).
448 There are a growing number of examples of intertidal organisms showing some level of

449 metabolic rate control or depression during warm temperature exposures, including the limpet *L.*
450 *digitalis* (Bjelde & Todgham 2013) which has an overlapping range with *L. austrodigitalis* in
451 Monterey Bay. Limpets from South Africa (Marshall & McQuaid 1991) and some intertidal
452 snails also exhibit metabolic rate control (McMahon & Russell-Hunter 1977, Sokolova et al.
453 2000, Marshall et al. 2011) in the range of warm daytime low tide temperatures, although the
454 response is not universal for intertidal gastropods (McMahon & Russell-Hunter 1977, McMahon
455 et al. 1995). Among the tropical species that exhibit metabolic rate depression, the magnitude of
456 that depression appears to be greater than that shown here by the temperate limpets, and it is
457 hypothesized that the more frequent and severe exposure to high temperatures in the tropics may
458 accentuate the need to control energy expenditures during prolonged emersion (Marshall et al.
459 2011). Even when there is evidence for metabolic rate control at moderate warm temperatures in
460 intertidal molluscs, Q_{10} values still tend to increase at the extreme limits of thermotolerance
461 (Marshall et al. 2011), as seen with all four limpet species measured here.
462 In the field, we observe a strong negative relationship between average daily maximum
463 temperature and algal fluorescence (F_o) on plates in different thermal microhabitats. The effect
464 of limpet grazing lowers algal density compared to grazer exclusion plates, but does not change
465 the negative relationship with increasing temperature. The greater amount of variability in F_o
466 values on "No grazer" plates may be due to a combination of factors related to plate location on
467 the shore, including exposure to sun or shading, wave splash, and the presence of small
468 opportunistic grazers such as *Littorina* snails that may have crawled through the mesh fence and
469 grazed the plates at some sites. Additionally, the consistent feeding of limpets on the grazed
470 plates may serve to mute the inherent variability in microalgal density along the shore. For the
471 limpets growing on those plates, the interacting effects of algal availability and temperature

472 across plates led to flat or slightly positive growth rates with increasing maximum temperature
473 and algal resources.

474 The observed increase in growth rates on warmer experimental plates, at least in the
475 presence of higher algal densities for *L. austrodigitalis* and *L. scabra*, supports the possibility of
476 a potential benefit to mild increases in low tide temperature above the predominant sea surface
477 temperature range. On the warmest plates measured here, limpets spent only 10% of the total
478 time at temperatures above 20 °C during the 24 week field experiment (Figure 1B shows
479 representative data for two *L. scabra* plates), and never exceeded the estimated CT_{max} limits for
480 any of the species. The predictions of increases in cumulative respired O_2 on the warmest plates
481 ranged from 5 to 14%, but the increased respiration did not manifest as significant decreases in
482 growth rate. The positive or neutral interactive effects of algal density with temperature on
483 limpet growth rates seem to outweigh the negative effects of increasing temperature alone. In
484 fully aquatic habitats, if there is sufficient food to support higher metabolic rates, growth rates
485 often increase (O'Connor 2009, Pangle & Peacor 2010, O'Regan et al. 2014), and the
486 combination of warmer waters and warmer low tide conditions between sites on the coast has
487 also been implicated in faster growth rates in mussels and other intertidal consumers (Phillips
488 2005, Blanchette et al. 2007). In the current experiment, where ocean temperature is consistent
489 across all of our microsites, we see evidence for positive effects of warmer low tide conditions
490 alone. However, it is important to reiterate that these low tide temperature conditions were
491 primarily non-stressful, and that low tide temperatures approaching the CT_{max} values of the
492 limpets species did not occur. Conditions on our temperate shoreline are only rarely stressful
493 enough to reach critical thermal maxima, in contrast to tropical sites where limpets and other
494 high shore grazers may routinely experience near-lethal temperatures (Williams & Morritt 1995,

Williams et al. 2005, Marshall et al. 2010, Dong et al. 2014), and so further warming in more stressful tropical regions will likely have predominantly negative effects.

There are several caveats to this general conclusion of beneficial effects of increased microalgal densities and warmer temperatures on limpet growth rates. All four limpet species graze microalgae and diatoms from the substratum, but the different thermal environments in our field experiment may drive differences in algal growth rate and species identity that could change the available energy for limpet growth (Castenholz 1961). Although we observed a general decline in algal density on plates with increasing temperature, we lack information on the species composition of the microalgal communities on the different plates, or their nutritional value. A second caveat is that our estimates of cumulative respiration are based only on rates for limpets at rest during a single acute exposure in air or seawater. Particularly following a high-temperature aerial exposure, the post-exposure period during the next high tide may bring prolonged increased respiration rates to accommodate an increased metabolic demand needed for the heat-shock response that drives repair or degradation of damaged proteins (Dong et al. 2008, Bjelde & Todgham 2013). There could also be a need to recover from anaerobic metabolism (Ellington 1983), though there is no evidence of anaerobic metabolic end product accumulation in *L. digitalis* from central California following aerial exposure (Bjelde & Todgham 2013). Due to these potential additional metabolic demands, our long-term estimates of cumulative respiration may underestimate the respired O_2, particularly on days when temperatures do reach stressful levels during low tide, although this makes the pattern of increased growth rate in warmer microsites all the more surprising. Finally, it should be noted that the limpets utilized in these experiments represent sub-adult and small adult size classes, but we have no performance information for smaller limpets. Smaller limpets should have higher mass-specific metabolic

518 rates and reduced energy stores relative to larger limpets, factors that may enhance the impacts of
519 emersed temperature stress on newly recruited individuals (Davies 1966, Kiørboe & Hirst 2014).
520 The thermal response curves measured here should be contrasted with the types of curves
521 typically reported for organisms such as lizards or insects (Angilletta 2009). The peak in
522 respiration we observe for limpet temperatures approaching 40 °C may have a different
523 interpretation than a thermal performance curve representing other metrics such as feeding rate,
524 locomotion speed, growth rate, or fecundity. For those other metrics, temperatures at the peak of
525 the performance curve might well be the most desirable place to spend time from the standpoint
526 of individual or population growth. In contrast, our measure of respiration rate, as a metric of
527 metabolic rate and calorie consumption, is somewhat removed from true measures of organismal
528 fitness. While we observe a peak in respiration at temperatures in the 32.5 to 37.5 °C range, it is
529 not clear those temperatures necessarily represent a true "performance peak" or "optimum",
530 particularly as temperatures in this range are known to induce a heat shock response in limpets
531 (Dong et al. 2008, Bjelde & Todgham 2013). Instead, for whole-organism fitness, limpet body
532 temperatures slightly below the range of peak respiration rates may be closer to an optimum
533 (Martin & Huey 2008), particularly if they avoid the risk and associated cost of a heat shock
534 response but allow for faster catabolic and anabolic rates.
535 *Lottia* limpets at HMS show a clear rise in respiration rate in response to rising body
536 temperature during aerial emersion, and a quick decline in respiration as they reach extreme high
537 temperatures that induce heat coma. The two high shore species, *L. scabra* and *L. austrodigitalis*,
538 maintain slightly lower respiration rates during intermediate temperatures in the 20 to 30 °C
539 range than their low shore counterparts, and have a higher CT_{max}, in line with the expectation
540 that the frequency and severity of high temperature exposures should be higher in the upper

541 littoral zone. In tracking growth over several months in the field, we see little evidence for
542 decreased growth in microhabitats with higher temperature variability and attendant higher peak
543 temperatures, despite estimated respiration demands being at least 5 to 14% higher, and in some
544 cases we observe increased growth rates in warmer sites when food is abundant. The relatively
545 short amount of total time encompassed by warm low tide exposures may have a small impact on
546 growth rates, but when the majority of those exposures avoid stressful extreme temperatures,
547 warmer microhabitats may be beneficial for intertidal consumers. Faster metabolic rates among
548 limpets could drive increased grazing effort at high tide to support greater metabolic demand and
549 increase growth rates, strengthening top-down control of microalgal density on the shore.
550 However, given the negative relationship between warmer low tide temperatures and microalgal
551 density observed in our grazer exclusion treatments, there is an opportunity for negative
552 feedback on limpet growth if algal growth rates cannot support increased grazing pressure from
553 limpets. Ultimately, the impacts of climate warming on energy transfer and growth rates in
554 intertidal habitats will be determined by this interaction between rising temperatures and species'
555 individual temperature responses that are likely optimized for intermediate temperature ranges.
556 The present day variation in temperature over small spatial scales in the intertidal (Denny et al.
557 2011) encompasses conditions that could increase growth rates in some instances, but continuing
558 warming of low tide aerial temperatures could begin to push organisms past their performance
559 optima.
560

Acknowledgements

This work was supported by NSF grant OCE-1131038 and 1130095 to B. J. Allen and M. W. Denny. We thank E. Duncan, J. McNamara, B. Pagan, T. Kroupa, and C. Prince for assistance in the setting up the experiments and assisting with field work.

Data Accessibility

Data related to this paper are deposited in the Stanford University Libraries Digital Repository at http://purl.stanford.edu/mz343tz6255. The project is registered with the NSF Biological and Chemical Oceanography Data Management Office (BCO-DMO; http://www.bco-dmo.org/) under grant numbers OCE-1131038 and OCE-1130095.

Literature cited

Allen BJ, Levinton JS (2014) Sexual selection and the physiological consequences of habitat choice by a fiddler crab. Oecologia 176:25-34

Angilletta MJ (2009) Thermal Adaptation: A Theoretical and Empirical Synthesis, Vol. Oxford University Press

Angilletta MJ, Huey RB, Frazier MR (2010) Thermodynamic effects on organismal performance: is hotter better? Physiol Biochem Zool 83:197-206

Barranguet C, Kromkamp J (2000) Estimating primary production rates from photosynthetic electron transport in estuarine microphytobenthos. Mar Ecol Prog Ser 204:39-52

Bayne BL, Scullard C (1978) Rates of feeding by *Thais (Nucella) lapillus* (L.). J Exp Mar Biol Ecol 32:113-129

582 Benson BB, Krause Jr D (1984) The concentration and isotopic fractionation of oxygen
583 dissolved in freshwater and seawater in equilibrium with the atmosphere. Limnol
584 Oceanogr 29:620-632
585 Bjelde B, Todgham A (2013) Thermal physiology of the fingered limpet *Lottia digitalis* under
586 emersion and immersion. J Exp Biol 216:2858-2869
587 Blanchette CA, Helmuth BST, Gaines SD (2007) Spatial patterns of growth in the mussel,
588 *Mytilus californianus*, across a major oceanographic and biogeograpic boundary at Point
589 Conception, California, USA. J Exp Mar Biol Ecol 340:126-148
590 Branch GM (1981) The biology of limpets: physical factors, energy flow, and ecological
591 interactions. Oceanogr Mar Biol, Annu Rev 19:235-380
592 Brett JR, Higgs DA (1970) Effect of temperature on the rate of gastric digestion in fingerling
593 sockeye salmon, *Oncorhynchus nerka*. J Fish Res Board Can 27:1767-1779
594 Castenholz RW (1961) Effect of grazing on marine littoral diatom populations. Ecology 42:783-
595 794
596 Collins LS (1976) Abundance, substrate angle, and desiccation resistance in two sympatric
597 species of limpets. Veliger 19:199-203
598 Craig PC (1968) The activity pattern and food habits of the limpet *Acmaea pelta*. Veliger 11:13-
599 19
600 Crummett L, Eernisse D (2007) Genetic evidence for the cryptic species pair, Lottia digitalis and
601 Lottia austrodigitalis and microhabitat partitioning in sympatry. Mar Biol 152:1-13
602 Davies PS (1966) Physiological ecology of *Patella*. I. The effect of body size and temperature on
603 metabolic rate. J Mar Biol Assoc U K 46:647-658

604 Davison AC, Hinkley DV (1997) Bootstrap methods and their application, Vol. Cambridge
605 University Press, Cambridge
606 Denny MW, Dowd WW, Bilir L, Mach KJ (2011) Spreading the risk: Small-scale body
607 temperature variation among intertidal organisms and its implications for species
608 persistence. J Exp Mar Biol Ecol 400:175-190
609 Denny MW, Harley CDG (2006) Hot limpets: predicting body temperature in a conductance-
610 mediated thermal system. J Exp Biol 209:2409-2419
611 Denny MW, Hunt LJH, Miller LP, Harley CDG (2009) On the prediction of extreme ecological
612 events. Ecol Monogr 79:397-421
613 Denny MW, Miller LP, Harley CDG (2006) Thermal stress on intertidal limpets: long-term
614 hindcasts and lethal limits. J Exp Biol 209:2420-2431
615 Deutsch CA, Tewksbury JJ, Huey RB, Sheldon KS, Ghalambor CK, Haak DC, Martin PR (2008)
616 Impacts of climate warming on terrestrial ectotherms across latitude. Proc Natl Acad Sci
617 USA 105:6668-6672
618 Diefenbach COdC (1975) Gastric function in *Caiman crocodilus* (Crocodylia: Reptilia)—I. Rate
619 of gastric digestion and gastric motility as a function of temperature. Comp Biochem
620 Physiol A 51:259-265
621 Dong Y-w, Han G-d, Huang X-w (2014) Stress modulation of cellular metabolic sensors:
622 interaction of stress from temperature and rainfall on the intertidal limpet *Cellana*
623 *toreuma*. Mol Ecol 23:4541-4554
624 Dong Y, Miller LP, Sanders JG, Somero GN (2008) Heat-shock protein 70 (Hsp70) expression
625 in four limpets of the genus *Lottia*: interspecific variation in constitutive and inducible
626 synthesis correlates with *in situ* exposure to heat stress. Biol Bull 215:173-181

627 Dong Y, Somero GN (2009) Temperature adaptation of cytosolic malate dehydrogenase of
628 limpets (genus *Lottia*): differences in stability and function due to minor changes in
629 sequence correlate with biogeographic and vertical distributions. J Exp Biol 212:169-177
630 Eaton CM (1968) The activity and food of the file limpet *Acmaea limatula*. Veliger 11:5-12
631 Ellington WR (1983) The recovery from anaerobic metabolism in invertebrates. J Exp Zool
632 228:431-444
633 Elliott J (1976) The energetics of feeding, metabolism and growth of brown trout (Salmo trutta
634 L.) in relation to body weight, water temperature and ration size. The Journal of Animal
635 Ecology 45:923-948
636 Elliott JM (1982) The effects of temperature and ration size on the growth and energetics of
637 salmonids in captivity. Comp Biochem Physiol B 73:81-91
638 Feder ME, Hofmann GE (1999) Heat-shock proteins, molecular chaperones, and the stress
639 response: evolutionary and ecological physiology. Annu Rev Physiol 61:243-282
640 Fly EK, Monaco CJ, Pincebourde S, Tullis A (2012) The influence of intertidal location and
641 temperature on the metabolic cost of emersion in *Pisaster ochraceus*. J Exp Mar Biol
642 Ecol 422-423:20-28
643 Fox J, Weisberg S (2011) An R Companion to Applied Regression, Vol. SAGE Publications,
644 Thousand Oaks, CA
645 Gilman SE (2006) Life at the edge: an experimental study of a poleward range boundary.
646 Oecologia 148:270-279
647 Hahn T, Denny M (1989) Tenacity-mediated selective predation by oystercatchers on intertidal
648 limpets and its role in maintaining habitat partitioning by *Collisella scabra* and *Lottia*
649 *digitalis*. Mar Ecol Prog Ser 53:1-10

650 Hawkins SJ, Hartnoll RG (1983) Grazing of intertidal algae by marine invertebrates. Oceanogr
651 Mar Biol, Annu Rev 21:195-282
652 Helmuth B (1999) Thermal biology of rocky intertidal mussels: quantifying body temperatures
653 using climatological data. Ecology 80:15-34
654 Hertz PE, Huey RB, Stevenson R (1993) Evaluating temperature regulation by field-active
655 ectotherms: the fallacy of the inappropriate question. Am Nat 142:796-818
656 Hochachka PW, Somero GN (2002) Biochemical Adaptation: Mechanism and Process in
657 Physiological Evolution, Vol. Oxford University Press, New York, USA
658 Hoekman D (2010) Turning up the heat: Temperature influences the relative importance of top-
659 down and bottom-up effects. Ecology 91:2819-2825
660 Honeywill C, Paterson D, Hagerthey S (2002) Determination of microphytobenthic biomass
661 using pulse-amplitude modulated minimum fluorescence. European Journal of Phycology
662 37:485-492
663 Huey RB (1991) Physiological consequences of habitat selection. Am Nat 137:S91-S115
664 Huey RB, Stevenson RD (1979) Integrating thermal physiology and ecology of ectotherms: A
665 discussion of approaches. Am Zool 19:357-366
666 Hunt LJH, Denny MW (2008) Desiccation protection and disruption: a trade-off for an intertidal
667 marine alga. J Phycol 44:1164-1170
668 Iles AC (2014) Towards predicting community level effects of climate: Relative temperature
669 scaling of metabolic and ingestion rates. Ecology 95:2657-2668
670 Jones NS (1948) Observations and experiments on the biology of *Patella vulgata* at Port St.
671 Mary, Isle of Man. Proc Trans Liverpool Biol Soc 56:60-77

672 Jones SJ, Mieszkowska N, Wethey DS (2009) Linking thermal tolerances and biogeography:
673 *Mytilus edulis* (L.) at its southern limit on the east coast of the United States. Biol Bull
674 217:73
675 Kiørboe T, Hirst AG (2014) Shifts in Mass Scaling of Respiration, Feeding, and Growth Rates
676 across Life-Form Transitions in Marine Pelagic Organisms. Am Nat 183:E118-E130
677 Kratina P, Greig HS, Thompson PL, Carvalho-Pereira TSA, Shurin JB (2012) Warming modifies
678 trophic cascades and eutrophication in experimental freshwater communities. Ecology
679 93:1421-1430
680 Kroeker KJ, Gaylord B, Hill TM, Hosfelt JD, Miller SH, Sanford E (2014) The role of
681 temperature in determining species' vulnerability to ocean acidification: A case study
682 using *Mytilus galloprovincialis*. PLoS ONE 9:e100353
683 Largen MJ (1967) The influence of water temperature upon the life of the dog-whelk *Thais*
684 *lapillus* (Gastropoda: Prosobranchia). J Anim Ecol 36:207-214
685 Maggi E, Jackson AC, Tolhurst T, Underwood AJ, Chapman MG (2013) Changes in
686 microphytobenthos fluorescence over a tidal cycle: implications for sampling designs.
687 Hydrobiologia 701:301-312
688 Marshall DJ, Dong Y-w, McQuaid CD, Williams GA (2011) Thermal adaptation in the intertidal
689 snail *Echinolittorina malaccana* contradicts current theory by revealing the crucial roles
690 of resting metabolism. J Exp Biol 214:3649-3657
691 Marshall DJ, McQuaid CD (1991) Metabolic rate depression in a marine pulmonate snail: pre-
692 adaptation for a terrestrial existence? Oecologia 88:274-276
693 Marshall DJ, McQuaid CD, Williams GA (2010) Non-climatic thermal adaptation: implications
694 for species' responses to climate warming. Biology Letters 6:669-673

695 Martin Tara L, Huey Raymond B (2008) Why "suboptimal" is optimal: Jensen's Inequality and
696 ectotherm thermal preferences. Am Nat 171:E102-E118
697 McMahon RF, Russell-Hunter WD (1977) Temperature relations of aerial and aquatic respiration
698 in six littoral snails in relation to their vertical zonation. Biol Bull 152:182-198
699 McMahon RF, Russell-Hunter WD, Aldridge DW (1995) Lack of metabolic temperature
700 compensation in the intertidal gastropods, *Littorina saxatilis* (Olivi) and *L. obtusata* (L.).
701 Hydrobiologia 309:89-100
702 Miller AC (1968) Orientation and movement of the limpet *Acmaea digitalis* on vertical rock
703 surfaces. Veliger 11:30-44
704 Miller LP (2013) The effect of water temperature on drilling and ingestion rates of the dogwhelk
705 *Nucella lapillus* feeding on *Mytilus edulis* mussels in the laboratory. Mar Biol 160:1489-
706 1496
707 Miller LP, Harley CDG, Denny MW (2009) The role of temperature and desiccation stress in
708 limiting the local-scale distribution of the owl limpet, *Lottia gigantea*. Funct Ecol 23:756-
709 767
710 Miller LP, Matassa CM, Trussell GC (2014) Climate change enhances the negative effects of
711 predation risk on an intermediate consumer. Glob Change Biol 20:3834-3844
712 Morelissen B, Harley CDG (2007) The effects of temperature on producers, consumers, and
713 plant-herbivore interactions in an intertidal community. J Exp Mar Biol Ecol 348:162-
714 173
715 Muggeo VMR (2008) segmented: an R package to fit regression models with broken-line
716 relationships. In: R News, Book 8

717 Muñoz JLP, Finke GR, Camus PA, Bozinovic F (2005) Thermoregulatory behavior, heat gain,
718 and thermal tolerance in the periwinkle *Echinolittorina peruviana* in central Chile. Comp
719 Biochem Physiol A 142:92-98
720 Murphy PC (1978) *Collisella austrodigitalis* sp. nov.: A sibling species of limpet (Acmaeidae)
721 discovered by electrophoresis. Biol Bull 155:193-206
722 O'Connor MI (2009) Warming strengthens an herbivore-plant interaction. Ecology 90:388-398
723 O'Connor MI, Piehler MF, Leech DM, Anton A, Bruno JF (2009) Warming and resource
724 availability shift food web structure and metabolism. PLoS Biol 7:e1000178
725 O'Regan SM, Palen WJ, Anderson SC (2014) Climate warming mediates negative impacts of
726 rapid pond drying for three amphibian species. Ecology 95:845-855
727 Pangle KL, Peacor SD (2010) Temperature gradients, not food resource gradients, affect growth
728 rate of migrating *Daphnia mendotae* in Lake Michigan. J Gt Lakes Res 36:345-350
729 Phillips NE (2005) Growth of filter-feeding benthic invertebrates from a region with variable
730 upwelling intensity. Mar Ecol Prog Ser 295:79-89
731 Pincebourde S, Sanford E, Casas J, Helmuth B (2012) Temporal coincidence of environmental
732 stress events modulates predation rates. Ecol Lett 15:680-688
733 Pincebourde S, Sanford E, Helmuth B (2008) Body temperature during low tide alters the
734 feeding performance of a top intertidal predator. Limnol Oceanogr 53:1562-1573
735 Pinheiro JC, Bates DM (2000) Mixed-effects models in S and S-PLUS, Vol. Springer Verlag,
736 New York
737 Pörtner HO (2012) Integrating climate-related stressor effects on marine organisms: unifying
738 principles linking molecule to ecosystem-level changes. Mar Ecol Prog Ser 470:273-290

739 R Development Core Team (2014) R: A language and environment for statistical computing. In.
740 R Foundation for Statistical Computing, Vienna, Austria
741 Rasband WS (1997-2014) ImageJ. In. U. S. National Institutes of Health, Bethesda, Maryland,
742 USA
743 Sanford E (1999) Regulation of keystone predation by small changes in ocean temperature.
744 Science 283:2095-2097
745 Sanford E (2002) Water temperature, predation, and the neglected role of physiological rate
746 effects in rocky intertidal communities. Integr Comp Biol 42:881-891
747 Sanford E, Menge BA (2001) Spatial and temporal variation in barnacle growth in a coastal
748 upwelling system. Mar Ecol Prog Ser 209:143-157
749 Serôdio J, Vieira S, Cruz S (2008) Photosynthetic activity, photoprotection and photoinhibition
750 in intertidal microphytobenthos as studied *in situ* using variable chlorophyll fluorescence.
751 Cont Shelf Res 28:1363-1375
752 Sokolova IM, Granovitch AI, Berger VJ, Johannesson K (2000) Intraspecific physiological
753 variability of the gastropod *Littorina saxatilis* related to the vertical shore gradient in the
754 White and North Seas. Mar Biol 137:297-308
755 Stich HB, Lampert W (1984) Growth and reproduction of migrating and non-migrating *Daphnia*
756 species under simulated food and temperature conditions of diurnal vertical migration.
757 Oecologia 61:192-196
758 Stillman JH (2002) Causes and consequences of thermal tolerance limits in rocky intertidal
759 porcelain crabs, genus *Petrolisthes*. Integr Comp Biol 42:790-796
760 Stillman JH (2003) Acclimation capacity underlies susceptibility to climate change. Science
761 301:65

762 Sutherland JP (1970) Dynamics of high and low populations of the limpet, *Acmaea scabra*
763 (Gould). Ecol Monogr 40:169-188
764 Tewksbury JJ, Huey RB, Deutsch CA (2008) Putting the heat on tropical animals. Science
765 320:1296-1297
766 Tomanek L (2002) The heat-shock response: its variation, regulation, and ecological importance
767 in intertidal gastropods (genus *Tegula*). Integr Comp Biol 42:797-807
768 Tomanek L, Somero GN (1999) Evolutionary and acclimation-induced variation in the heat-
769 shock responses of congeneric marine snails (Genus *Tegula*) from different thermal
770 habitats: implications for limits of thermotolerance and biogeography. J Exp Biol
771 202:2925-2936
772 Tomanek L, Zuzow MJ (2010) The proteomic response of the mussel congeners Mytilus
773 galloprovincialis and M-trossulus to acute heat stress: implications for thermal tolerance
774 limits and metabolic costs of thermal stress. J Exp Biol 213:3559-3574
775 Walker CG (1968) Studies on the jaw, digestive system, and coelomic derivatives in
776 representatives of the genus *Acmaea*. Veliger 11:88-97
777 Williams GA, De Pirro M, Leun KM, Morritt D (2005) Physiological responses of heat stress on
778 a tropical shore: the benefits of mushrooming behaviour in the limpet *Cellana grata*. Mar
779 Ecol Prog Ser 292:213-224
780 Williams GA, Morritt D (1995) Habitat partitioning and thermal tolerance in a tropical limpet,
781 *Cellana grata*. Mar Ecol Prog Ser 124:89-103
782 Wolcott TG (1973) Physiological ecology and intertidal zonation in limpets (*Acmaea*): a critical
783 look at limiting factors. Biol Bull 145:389-422

784 Woodin SA, Hilbish TJ, Helmuth B, Jones SJ, Wethey DS (2013) Climate change, species
785 distribution models, and physiological performance metrics: predicting when
786 biogeographic models are likely to fail. Ecol Evol 3:3334-3346
787 Yamane L, Gilman SE (2009) Opposite responses by an intertidal predator to increasing aquatic
788 and aerial temperatures. Mar Ecol Prog Ser 393:27-36

789

790

791

Tables

Table 1. Estimated respiration break points and median heat coma temperatures (CT_{max}) for limpets held in air, with temperatures raised from 15 °C to a target temperature at 10 °C h^{-1} and held for 2 h. Because the peak respiration for *L. scabra* occurred at 37.5 °C, it was not possible to estimate a break point via piecewise regression from the single temperature above the peak.

Species	Respiration break point temperature (°C, ± 1SE)	Critical Thermal Maximum (°C, ± 1SE)
L. scabra	NA	39.6 (± 0.9)
L. austrodigitalis	34.2 (± 1.0)	38.8 (± 0.5)
L. limatula	36.5 (± 0.4)	36.9 (± 0.5)
L. pelta	34.4 (± 0.4)	34.6 (± 0.4)

800

801 Table 2. Linear mixed effects model summary for limpet growth rate (mg day^{-1}). Average daily
802 maximum temperature during a census period, algal density (log-transformed dark-adapted
803 fluorescence, F_o) at the start of a census period, and limpet species were treated as fixed factors.
804 Random effects included log-transformed algal density, experimental plates, and individual
805 limpets nested within experimental plates in order to account for nesting and repeated measures
806 through time. The model accounts for first order autocorrelation among repeated measures using
807 an AR(1) autoregressive structure.

Treatment	numDF	denDF	*F*	*P*
Average Daily Maximum (°C)	1	671	20.36	<0.001
Algae density, Log (F_o)	1	671	17.20	<0.001
Species	3	44	1.63	0.196
Avg. Daily Max. × Algae density	1	671	37.50	<0.001
Avg. Daily Max. × Species	3	671	4.84	0.002
Algae density × Species	3	671	3.16	0.024
Avg. Daily Max. × Algae density × Species	3	671	8.12	<0.001

808

809

Table 3. Temperature statistics for the single coolest and single warmest plate containing each limpet species in the field, and estimated cumulative respiration on the coolest and warmest plate over the course of the experiment from June to December 2013.

	Cool Plate			Warm Plate			
Species	Average daily temperature range, °C	Maximum temperature, °C	Estimated cumulative respired oxygen, µmol	Average daily temperature range, °C	Maximum temperature, °C	Estimated cumulative respired oxygen, µmol	Estimated respiration increase
L. scabra	3.3	26.0	1150	10.6	35.0	1314	14.3%
L. austrodigitalis	2.9	23.0	1383	8.5	36.5	1456	5.3%
L. limatula	2.4	21.5	2520	7.8	34.5	2732	8.4%
L. pelta	2.9	24.5	2148	8.2	33.5	2363	10.0%

Figure legends

Figure 1. A) A hypothetical temperature-performance curve, where some metric of performance (grazing rate, growth rate, etc.) climbs with increasing temperature towards a peak or plateau, and then drops off quickly as temperatures increase further. B) Kernel density estimates of limpet body temperatures from June through December 2013 at cool and warm microsites on the high shore at HMS (1.7 m above Mean Lower Low Water). The gray hatched region indicates the approximate portion of time spent at temperatures between 16.6 and 28 °C, which are above the warmest ocean temperature at the site, but below the range that typically induces a heat shock response in Lottia limpets (Dong et al. 2008). The solid gray region above 28 °C represents the temperature *range* where most Lottia exhibit a heat shock response. The samples include 3,939 hours of data at two sites collected at 12 minute intervals, with the kernel bandwidth set at 0.6.

Figure 2. A) *Lottia* limpets from central California. B) *L. scabra* and *L. austrodigitalis* are found in the high intertidal zone, *while L.* limatula *and L.* pelta are found in the low to middle intertidal zone.

Figure 3. Respiration rates in air and seawater, and aerial respiration Q_{10} values for *Lottia* limpets. (A) *Lottia* limpet mass-specific aerial respiration rates (closed symbols) and aquatic respiration rates (open symbols) with 95% confidence intervals. The horizontal positions of the points have been staggered, but trials occurred at the temperatures indicated on the horizontal axis (n = 12 limpets per temperature). (B) Aerial respiration Q_{10} values for each temperature range, with bootstrapped 95% confidence intervals back-transformed from log-transformed samples. The upper confidence limit for *L. scabra* in the 10-15 °C range (= 10.3) is cut off to improve the clarity of the plotted values.

838 Figure 4. Algae dark adapted fluorescence, F_o (a proxy for algal density), on experimental plates
839 versus limpet species treatment and average daily maximum temperature in the time period
840 preceding each of six census dates between June and December 2013. Fitted lines *are* back-
841 transformed estimates from models fitted with *log-transformed* F_o values.

842 Figure 5. Partial regression slopes (± 95% confidence limits shown in grey) from the linear
843 model of limpet growth rate versus average daily maximum temperature during a census period,
844 algal density (log F_o) at the start of a census period, and limpet species. Individual panels
845 illustrate the fitted relationship between average daily maximum temperature (°C) and limpet
846 growth rate (mg day-1), for each limpet species (rows) at 3 representative algal density values
847 (left column, F_o = 25; center, F_o = 50; right column, F_o = 75). The rug of points on the horizontal
848 axis represents the distribution of average daily maximum temperature values in the dataset.

849 Figure 6. Estimated respiration rates for an average size *L. scabra* (18.5 mg dry tissue mass)
850 living on the single warmest (red) and single coolest (blue) plate in the field experiment. A)
851 Temperature records for the warmest *and coolest* plates in the field that held L. *scabra*. B).
852 Estimated respiration rates for L. scabra on the warmest and coolest plates. A close up view of
853 the three day time period represented by the grey box in (B) is shown in (C), along with the
854 corresponding tides.

855

Figures

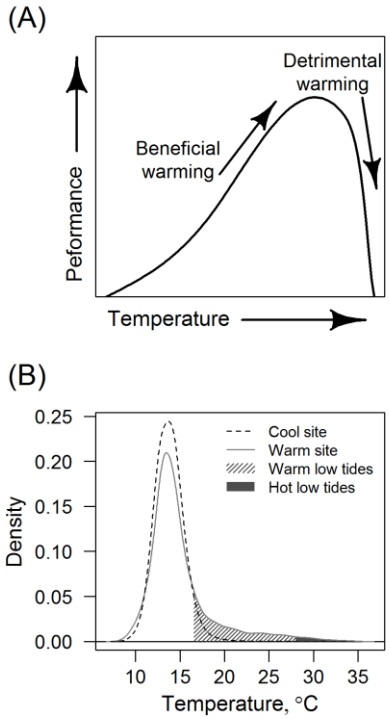

Figure 1. A) A hypothetical temperature-performance curve, where some metric of performance (grazing rate, growth rate, etc.) climbs with increasing temperature towards a peak or plateau, and then drops off quickly as temperatures increase further. B) Kernel density estimates of limpet body temperatures from June through December 2013 at cool and warm microsites on the high shore at HMS (1.7 m above Mean Lower Low Water). The gray hatched region indicates the approximate portion of time spent at temperatures between 16.6 and 28 °C, which are above the warmest ocean temperature at the site, but below the range that typically induces a heat shock response in *Lottia* limpets (Dong et al. 2008). The solid gray region above 28 °C represents the temperature range where most *Lottia* exhibit a heat shock response. The samples include 3,939 hours of data at two sites collected at 12 minute intervals, with the kernel bandwidth set at 0.6.

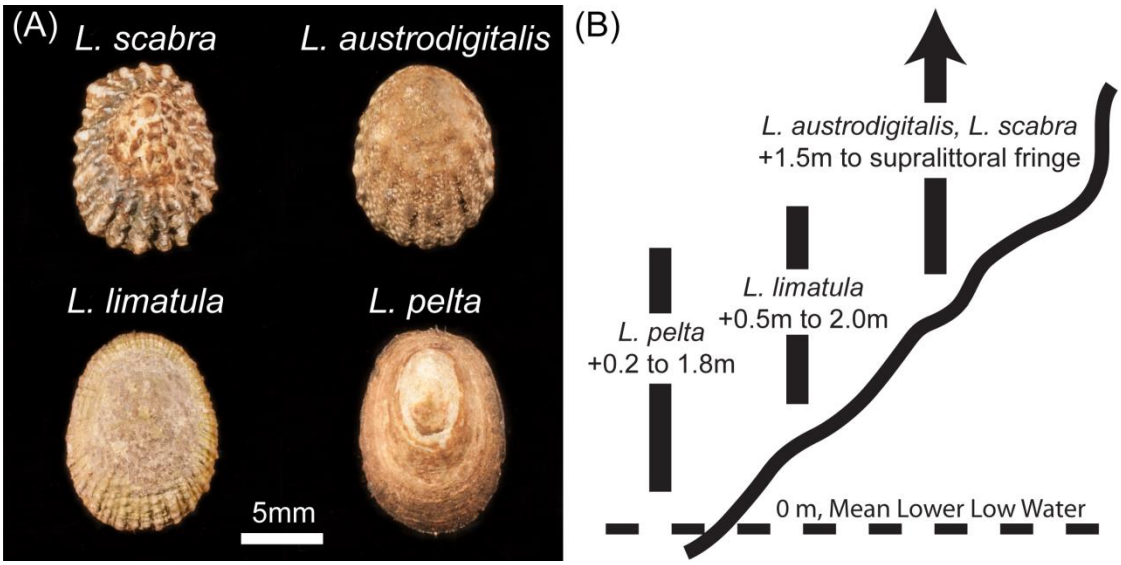

868

869 Figure 2. A) *Lottia* limpets from central California. B) *L. scabra* and *L. austrodigitalis* are found

870 in the high intertidal zone, while *L. limatula* and *L. pelta* are found in the low to middle intertidal

871 zone.

872

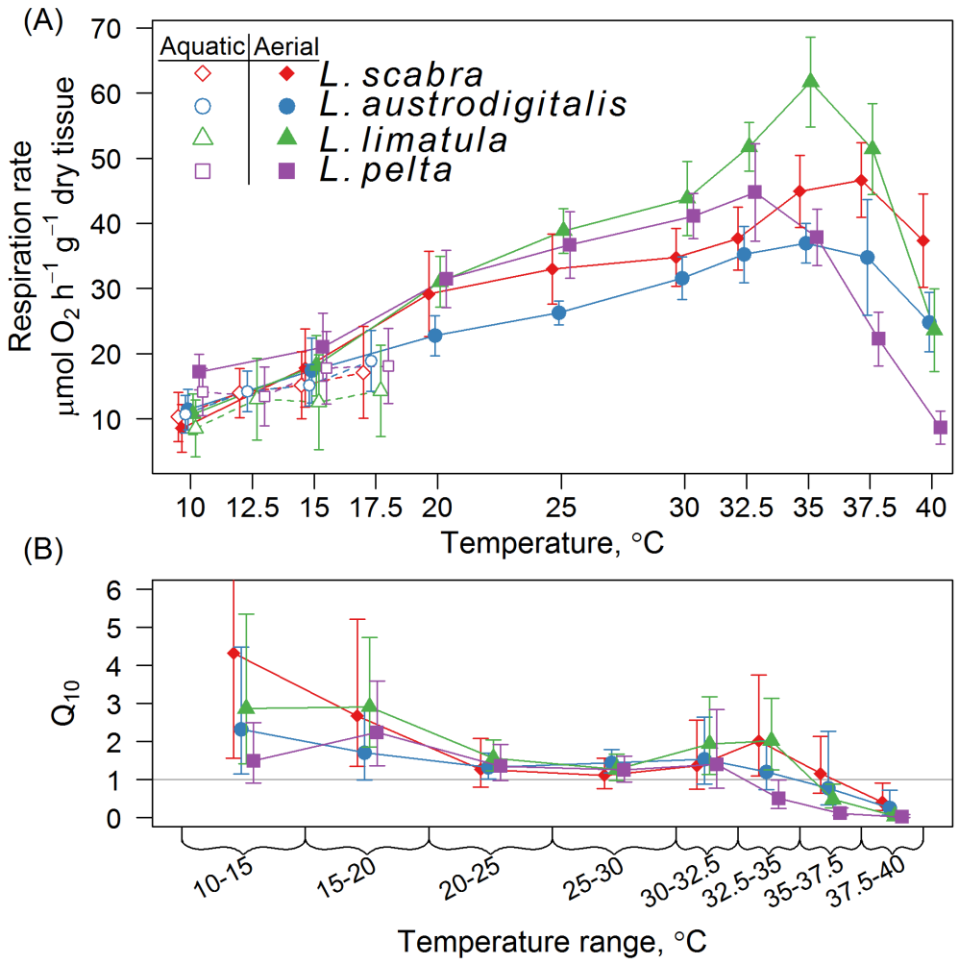

873

874 Figure 3. Respiration rates in air and seawater, and aerial respiration Q_{10} values for *Lottia*
875 limpets. (A) *Lottia* limpet mass-specific aerial respiration rates (closed symbols) and aquatic
876 respiration rates (open symbols) with 95% confidence intervals. The horizontal positions of the
877 points have been staggered, but trials occurred at the temperatures indicated on the horizontal
878 axis (n = 12 limpets per temperature). (B) Aerial respiration Q_{10} values for each temperature
879 range, with bootstrapped 95% confidence intervals back-transformed from log-transformed
880 samples. The upper confidence limit for *L. scabra* in the 10-15 °C range (= 10.3) is cut off to
881 improve the clarity of the plotted values.

882

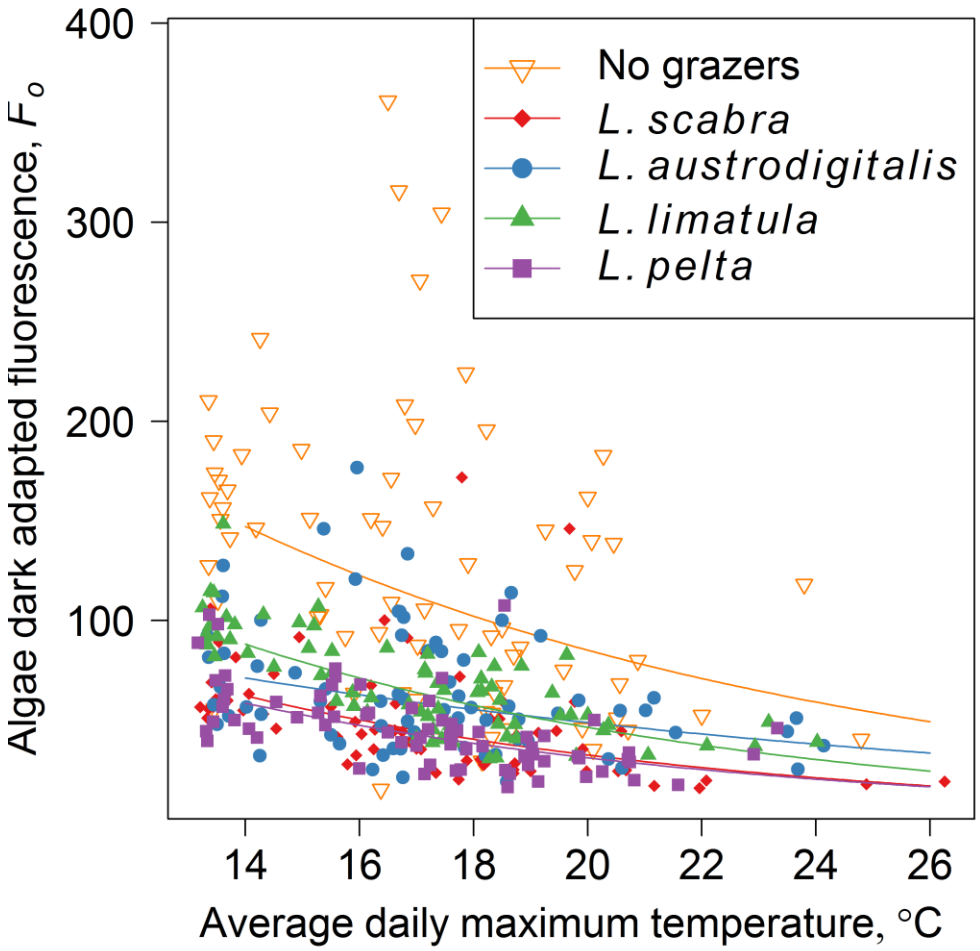

883

884 Figure 4. Algae dark adapted fluorescence, F_o (a proxy for algal density), on experimental plates
885 versus limpet species treatment and average daily maximum temperature in the time period
886 preceding each of six census dates between June and December 2013. Fitted lines are back-
887 transformed estimates from models fitted with log-transformed F_o values.

888

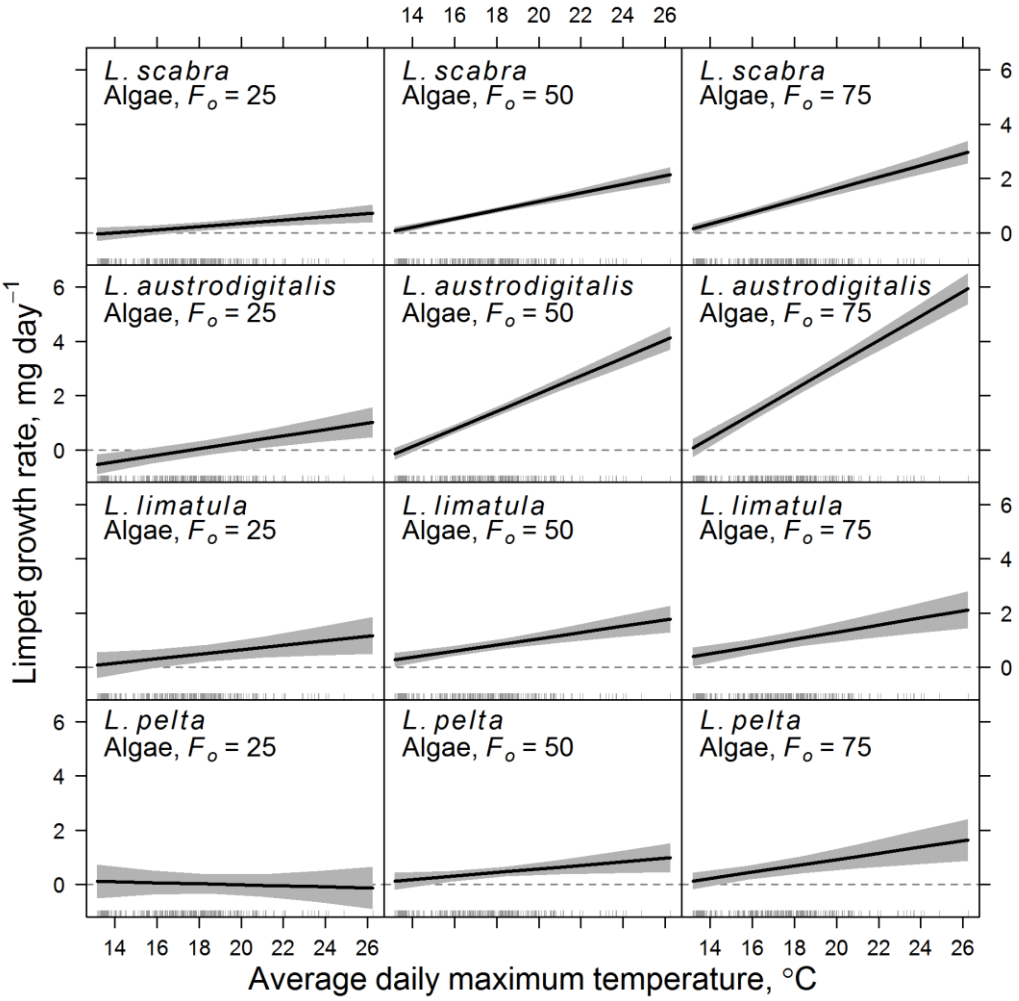

889

890 Figure 5. Partial regression slopes (± 95% confidence limits shown in grey) from the linear
891 model of limpet growth rate versus average daily maximum temperature during a census period,
892 algal density (log F_o) at the start of a census period, and limpet species. Individual panels
893 illustrate the fitted relationship between average daily maximum temperature (°C) and limpet
894 growth rate (mg day^{-1}), for each limpet species (rows) at 3 representative algal density values
895 (left column, F_o = 25; center, F_o = 50; right column, F_o = 75). The rug of points on the horizontal
896 axis represents the distribution of average daily maximum temperature values in the dataset.

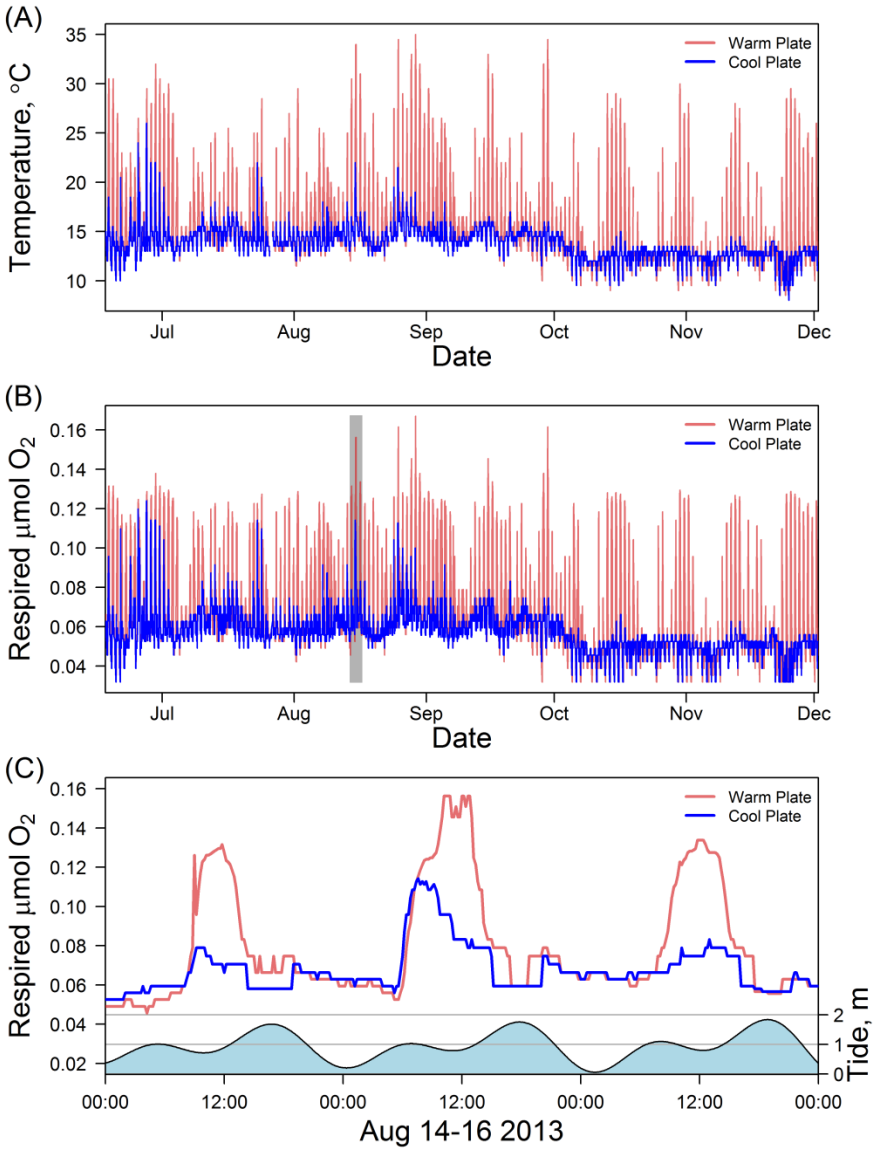

897

898 Figure 6. Estimated respiration rates for an average size *L. scabra* (18.5 mg dry tissue mass)
899 living on the single warmest (red) and single coolest (blue) plate in the field experiment. A)
900 Temperature records for the warmest and coolest plates in the field that held *L. scabra*. B).
901 Estimated respiration rates for *L. scabra* on the warmest and coolest plates. A close up view of
902 the three day time period represented by the grey box in (B) is shown in (C), along with the
903 corresponding tides.

904

905 **Supplemental Tables**

906 Table S1. Dry tissue mass (mg) distributions of limpets used in the aerial and aquatic respiration

907 trials (n = 12 per species per temperature).

Species	Mean dry tissue mass, mg (± 1SD)	Minimum tissue mass, mg	Maximum tissue mass, mg
L. scabra	23.1 (± 9)	6.8	49.1
L. austrodigitalis	29.0 (± 10)	12.0	63.7
L. limatula	43.0 (± 20)	11.2	117.5
L. pelta	32.5 (± 11)	12.3	69.7

908

909

910 Table S2. Results of generalized least squares model of log-transformed dark-adapted algal
911 fluorescence values (F_o) versus average daily maximum temperature and limpet species
912 (including the No Grazer treatment). The model included an AR(1) correlation structure for the
913 Date of each reading ($\varphi = 0.23$).

914

	numDf	denomDF	*F*	*P*
Intercept	1	350	21,225.4	< 0.001
Avg. daily maximum temperature	1	350	104.3	< 0.001
Species	4	350	80.8	< 0.001
Avg. daily maximum × Species	4	350	1.89	0.111

915

916

Table S3. Treatment contrast coefficient estimates for the generalized least squares model of $\log_e$-transformed dark-adapted algal fluorescence values (F_o) versus average daily maximum temperature and limpet species (including the No Grazer treatment). The No Grazer treatment is the reference level.

Coefficient	Estimate	Std. Error	*t*-value	*P*
Intercept	6.422	0.327	19.73	<0.001
Average daily maximum temperature	-0.100	0.019	-5.32	<0.001
L. scabra	-0.722	0.425	-1.70	0.091
L. austrodigitalis	-1.402	0.446	-3.15	0.002
L. limatula	-0.411	0.442	-0.93	0.353
L. pelta	-0.746	0.434	-1.72	0.086
Avg. daily max. × *L. scabra*	-0.013	0.024	-0.52	0.607
Avg. daily max. × *L. austrodigitalis*	0.043	0.026	1.67	0.097
Avg. daily max. × *L. limatula*	-0.010	0.026	-0.39	0.698
Avg. daily max. × *L. pelta*	-0.015	0.025	-0.58	0.565

924 Table S4. Coefficients for regressions of the form $Y = \alpha X^{\beta}$ for limpet dry tissue mass or shell
925 mass (mg) versus shell projected area (mm^2) when viewed from overhead. R^2 for linear fits to log
926 transformed data are given, along with sample size *n* for each species.

	Dry tissue mass			Shell mass			
Species	α	β	R^2	α	β	R^2	n
L. scabra	0.0435	1.36	0.75	0.100	1.62	0.87	247
L. austrodigitalis	0.0376	1.41	0.83	0.132	1.55	0.80	242
L. limatula	0.0350	1.40	0.90	0.103	1.56	0.87	227
L. pelta	0.1100	1.21	0.85	0.177	1.46	0.88	245

927

Table S5. Treatment contrast coefficient estimates for the linear mixed effects model of limpet growth rate (mg day^{-1}) with average daily maximum temperature during each census period, log_e-transformed algal density (F_o) at the beginning of each census period, and limpet species as fixed factors. The random effects included log_e-transformed F_o, an effect for plate (standard deviation of intercept = 2.23, log(F_o) = 0.60), and for individual limpets nested within plates to account for the repeated measures of limpets through time (standard deviation of intercept = 0.99, log(F_o) = 0.28, residual = 0.74). First order autocorrelation among the repeated limpet measures through time is accounted for using an AR(1) autoregressive correlation structure (φ = 0.22). The estimate for *L. scabra* is the reference level in the model. The model was fit using the *nlme* package (Pinheiro and Bates, 2000).

Coefficient	Estimate	Std. Error	df	*t*-value	*P*
Intercept	8.865	2.508	671	3.535	<0.001
Average daily maximum temperature, °C	-0.847	0.133	671	-6.382	<0.001
Log (F_o)	-3.402	0.650	671	-5.231	<0.001
L. austrodigitalis	-8.846	4.056	44	-2.181	0.035
L. limatula	-3.350	4.245	44	-0.789	0.434
L. pelta	-4.779	4.293	44	-1.113	0.272
Avg. daily max. × Log(F_o)	0.300	0.035	671	8.684	<0.001
Avg. daily max. × *L. austrodigitalis*	0.785	0.219	671	3.581	<0.001
Avg. daily max. × *L. limatula*	0.435	0.233	671	1.868	0.062
Avg. daily max. × *L. pelta*	0.569	0.242	671	2.352	0.019
Log(F_o) × *L. austrodigitalis*	3.085	1.040	671	2.966	0.003
Log(F_o) × *L. limatula*	1.802	1.053	671	1.711	0.088
Log(F_o) × *L. pelta*	1.948	1.150	671	1.694	0.091
Avg. daily max. × Log(F_o) × *L. austrodigitalis*	-0.255	0.057	671	-4.504	<0.001
Avg. daily max. × Log(F_o) × *L. limatula*	-0.178	0.059	671	-3.018	0.003
Avg. daily max. × Log(F_o) × *L. pelta*	-0.197	0.066	671	-2.983	0.003